5852–5866 *Nucleic Acids Research, 2019, Vol. 47, No. 11* *Published online 13 May 2019*
doi: 10.1093/nar/gkz371

Myg1 exonuclease couples the nuclear and mitochondrial translational programs through RNA processing

Ritika Grover[1,2,†], Shaunak A. Burse[1,2,†], Shambhavi Shankrit[1], Ayush Aggarwal[1,2], Kritika Kirty[3], Kiran Narta[1], Rajpal Srivastav[1], Ashwini Kumar Ray[4], Garima Malik[1], Archana Vats[1], Rajender K. Motiani[1], Lipi Thukral[1], Soumya Sinha Roy[1], Sudha Bhattacharya[4], Rakesh Sharma[1], Krishnamurthy Natarajan[3], Mitali Mukerji[1], Rajesh Pandey[1], Rajesh S. Gokhale[1,5] and Vivek T. Natarajan[1,2,*]

[1]CSIR-Institute of Genomics and Integrative Biology, Mathura Road, New Delhi, India, [2]Academy of Scientific and Innovative Research, Rafi Marg, New Delhi, India, [3]School of Life Sciences, Jawaharlal Nehru University, New Delhi, India, [4] School of environmental Sciences, Jawaharlal Nehru University, New Delhi, India and [5]National Institute of Immunology, Aruna Asaf Ali Marg, New Delhi, India

Received September 12, 2018; Revised April 12, 2019; Editorial Decision April 15, 2019; Accepted April 30, 2019

ABSTRACT

Semi-autonomous functioning of mitochondria in eukaryotic cell necessitates coordination with nucleus. Several RNA species fine-tune mitochondrial processes by synchronizing with the nuclear program, however the involved components remain enigmatic. In this study, we identify a widely conserved dually localized protein Myg1, and establish its role as a 3′-5′ RNA exonuclease. We employ mouse melanoma cells, and knockout of the Myg1 ortholog in *Saccharomyces cerevisiae* with complementation using human Myg1 to decipher the conserved role of Myg1 in selective RNA processing. Localization of Myg1 to nucleolus and mitochondrial matrix was studied through imaging and confirmed by sub-cellular fractionation studies. We developed *Silexoseqencing*, a methodology to map the RNAse trail at single-nucleotide resolution, and identified *in situ* cleavage by Myg1 on specific transcripts in the two organelles. In nucleolus, Myg1 processes pre-ribosomal RNA involved in ribosome assembly and alters cytoplasmic translation. In mitochondrial matrix, Myg1 processes 3′-termini of the mito-ribosomal and messenger RNAs and controls translation of mitochondrial proteins. We provide a molecular link to the possible involvement of Myg1 in chronic depigmenting disorder vitiligo. Our study identifies a key component involved in regulating spatially segregated organellar RNA processing and establishes the evolutionarily conserved ribonuclease as a coordinator of nucleo-mitochondrial crosstalk.

INTRODUCTION

Eukaryotic cell harbours two interdependent genomes encoded by the nucleus and mitochondria, which need to constantly communicate to balance energy needs and oxidative state of the cell. Molecular players that localize dually to both nucleus and mitochondria could mediate this synchrony. While the nuclear encoded proteins are synthesized in the cytoplasm, polypeptides encoded by the mitochondria are translated in the mitochondrial matrix. These proteins are assembled into five oxidative phosphorylation (OXPHOS) complexes within the mitochondrial inner membrane. Central transcriptional coactivators PGC1-α and β modulate the expression of nuclear genes and control mitochondrial respiratory capacity of the cell (1). Multigenic transcripts arising out of mitochondrial genome requires several nuclear factors to process the RNA (2). Thus the nuclear genome encodes majority of mitochondrial proteins and the acquired endo-symbiont is primarily governed by the nucleus. Often these homeostatic communications are altered leading to the manifestation of disease phenotypes in complex disorders. A common outcome of this dysregulation is elevated oxidative stress levels due to Reactive Oxygen Species (ROS). Which is observed in diseases such

*To whom correspondence should be addressed. Tel: +91 11 29879203; Email: tnvivek@igib.in
†The authors wish it to be known that, in their opinion, the first two authors should be regarded as Joint First Authors.
Present address: Rajesh S. Gokhale, Immunometabolism Lab, National Institute of Immunology, Aruna Asaf Ali Marg,New Delhi - 110067, India

as diabetes, neurodegenerative disorders and vitiligo, an acquired depigmenting disorder of the skin.

Translational machinery of cells, the ribosomes, comprise of intricately packed assemblies of ribonucleic acids and proteins. These megasynthases decode the mRNA message during translation. Biogenesis of ribosomes is a multistep process that comprises synthesis of ribosomal RNAs and their complex processing, which is followed by assembly of pre-ribosomal subunits (3). For the cytoplasmic ribosomes, this process begins at nucleolus and continues in the cytoplasm where the ribonucleoprotein complexes are finally assembled. A similar process is operational in the mitochondrial matrix wherein mitoribosomes are assembled from nuclear encoded proteins and the mitochondria encoded ribosomal RNAs (4). Nuclear rRNA processing involves removal of external transcribed sequences (5′ETS and 3′ETS) and internal transcribed sequences (ITS-1 and ITS-2) from precursor rRNAs (pre-rRNAs) to form mature 18S, 5.8S and 28S rRNAs. This cleavage and processing is mediated by both endonucleases and exonucleases (5). However, the complete mapping of processing sites and identification of enzymes involved in multiple cleavage events is still being elucidated. Details of the mitochondrial RNA processing are only beginning to emerge (6,7).

The translational machinery in nucleo-cytoplasmic compartments and the mitochondria work in synchrony. This is evident when cells swiftly adapt to environmental cues such as the prevailing nutritional status (8). Adaptation of yeast cells to glycerol induces rapid and coordinated expression of mitochondrial genes in the two compartments. This study shows that the levels of OXPHOS transcripts encoded in nucleus and mitochondria do not increase concordantly, instead the two translational events are expeditiously regulated and coupled. Hence the nuclear genome coordinates the two translational programs for the timely synthesis of oxidative phosphorylation complexes. A comprehensive understanding of the synchrony is possible only upon identification of factors and mechanisms that bring about concordant changes in nucleus and mitochondria. Synthesis of multigenic mitochondrial transcripts encoding messenger, ribosomal and transfer RNA renders RNA dynamics as an excellent frontier to fine-tune not just the messenger RNA but also the translational capacity within mitochondria.

The RNA metabolism, in mitochondria is in spotlight with the identification of numerous proteins associated with RNA granules in the matrix (9,10), These proteins modulate processing of heavy, heavy short and light transcripts encoded by the mitochondrial genome (11). Recent advances have identified the role of MRPP and Elac2 endonucleases in cleaving tRNA molecules that intercept mRNA and rRNA genes of mitochondria (12,13). Quest for an RNA exonuclease in mammalian mitochondria is long standing. PNPT1 was thought to mediate RNA degradation, but its localization to the intermembrane space (IMS) and nuclease-independent role in RNA import limits the possibility in RNA turnover (14). Lately, it was shown that IMS localized PNPT1 is released into cytosol upon mitochondrial outer membrane permeabilization and cleaves poly(A) RNAs leading to apoptosis (15). Recent discovery of EXD2 exonuclease, in the mitochondrial matrix, has resulted in the identification of its role in mitoribosomal translational integrity (16). This enzyme prevents premature translation of mRNA from pre-ribosomal structures by exonucleolytic cleavage. Pde12 is another such deadenylase that plays a crucial role in mitochondrial mRNA stability and mitochondrial translation (17). Functional genomic tools for RNA processing components in mitochondria have facilitated the identification and validation of genes involved in mitochondrial functionality (2,18). Development of Parallel Analysis of RNA End (PARE)-sequencing enabled the identification of target sites for the endonucleases involved in mitochondrial RNA processing (2).

Despite these advances, our understanding of RNA dynamics in mitochondria is inadequate and many of the components of mitochondrial RNA metabolism still remain to be identified. Harmonized functioning of mitochondria with nucleus would require parallel processing of RNA, to ensure rapid synchrony between the two organelles. In this study, we characterize a novel exonuclease Myg1, belonging to the conserved UPF0160 superfamily. Myg1 localizes to both nucleus and mitochondria, where it processes ribosomal RNAs encoded by both the genomes. Myg1 is also involved in the turnover of nuclear and mitochondrial mRNA, thereby altering the message as well as the translational machinery for coordination. Myg1 expression is altered in vitiligo, and changes in the transcriptome suggest Myg1 footprint. We demonstrate that Myg1 governs mitochondrial functions. Its alteration in vitiligo could explain mitochondrial dysfunction observed in this chronic disorder which needs to be further investigated. Thereby, our systematic analysis unravels a hitherto unknown player involved in nucleo-mitochondrial cross-talk conserved across evolution.

MATERIALS AND METHODS

Nuclease enzyme activity assays

Exonuclease activity of Myg1 was performed with long synthetic radiolabeled or fluorescently labelled oligonucleotides as substrates. 35 mer DNA and RNA oligonucleotides, phosphodiester bonded or interspersed with Locked Nucleic Acid (LNA) modifications were 5′ end-labeled with [γ-^{32}P] ATP or FAM and were used as substrates (sequence of the oligonucleotides in Supplementary Table S3). For the double stranded DNA the labelled single stranded oligonucleotides were annealed with the corresponding unlabeled antisense oligonucleotides. The exonuclease activity assay was carried out by incubating (280 nM) of 5′-end-labeled ssDNA or RNA with 10 μg of purified Myg1 protein in 20 mM Tris–HCl, pH 7.5, 100 mM KCl, 10 mM $MgCl_2$ or $MnCl_2$ and 1 mM dithiothreitol (DTT) at 37°C for different time periods. The exonuclease activity was terminated by addition of 50 mM EDTA and heating the reaction mix at 95°C for 15 min. The products were analysed on 15% polyacrylamide gel containing 8 M urea and visualized on a Phosphor-Imager (Bio-Rad).

Silenced exonuclease sequencing (Silexoseq)

Experimental design: To map the trail of exonuclease on RNA transcripts, we designed an approach to perform the Silencing of Exonuclease followed by RNA Sequencing

(Silexoseq). This method compares sequencing reads in exonuclease silenced and control conditions and involves organelle enrichment prior to RNA isolation and sequencing. This is performed to avoid, mitochondrial pseudogene encoded transcripts in the nucleus. In this sequencing method the total RNA is taken up for the library preparation without polyA enrichments, size fractionation or rRNA cleavages to enrich for unprocessed, less abundant intermediates. The depth of sequencing is high with average of FPKM per transcript ranging from around 2 to 100. Transcript specific depth of sequencing is close to 5 one-end reads per million reads. This is rendered possible due to organelle enrichments. The analysis design involves sequence analysis and representation of the data as fold change over control at every base position, which is typically not possible with routine RNA seq reads due to depth issues.

Myg1 exonuclease was silenced in the B16 cells by SMARTpool:ON-TARGETplus Myg1 siRNA, L-055338-01-0005. This was followed by isolation of mitochondria and nucleus via cell fractionation. Total RNA was isolated from these compartments and library was prepared according to manufacturers instructions without RNA size fractionation to ensure capturing shorter fragments of RNA (Illumina TrueSeq RNA library Prep V2). Details of the procedure are given below:

RNA isolation from nucleus and mitochondria: The whole RNA was isolated from the control and Myg1 siRNA transfected B16 cells (SMARTpool:ON-TARGETplus Myg1 siRNA, L-055338-01-0005) and the knockdown was independently validated using western blot analysis of Myg1. Nuclear RNA was isolated using the Norgen's nuclear and cytoplasmic RNA isolation kit (Norgen Biotek Corp.) as per manufacturer's guidelines. Mitochondria were isolated using Qproteome mitochondria isolation kit (Qiagen) and RNA was isolated using total RNA isolation kit (Qiagen).

RNA library preparations: TruSeq-RNA Sample Preparation V2 kit from Illumina was used to prepare libraries for sequencing mouse mitochondrial and the nuclear RNA. Briefly 1 μg of total RNA was taken for the library preparation, it was purified and fragmented. This was followed by cDNA synthesis in two steps using random hexamers and end repairing as per manufacturer's protocol. A single 'A' nucleotide was added to the 3′ ends of the blunt fragments to prevent them from ligating to one another during the adapter ligation reaction. Subsequent adaptor ligation was done which was followed by PCR based enrichment of the samples for the preparation of library. The final libraries were then quantified and checked for the quality as per True Seq-RNA Sample preparation V2 kit protocol. From the manufacturers protocol the poly-A binding step was omitted and used total RNA to start the protocol form the Elute-Prime-Fragment step. The entire library was taken without size fractionation for sequencing. The clusters for the library samples were generated using Truseq PE cluster kit v3 cBOT HS and each library was ran on a lane of flowcell on Hiseq 2000 (TruSeq SBS Kit v3 HS 200 cycles) and the paired end sequences of 100 base pair (bp) were generated.

Initial QC: For the analysis of reads, quality assessment was performed using FastQC (https://www.bioinformatics.babraham.ac.uk/projects/fastqc/). The bad quality reads were filtered using Trimmomatic (Version 0.35) with SLIDINGWINDOW of 4:20 and MINLEN of 25.

Alignment: Alignment was performed against the reference genome NC_005089.1 for the mitochondrial reads and Rn45s (45s pre-ribosomal RNA) Gene ID: X82564.1 for the nuclear reads using Bowtie2 (version 2.2.9) (with default parameters). Post-processing analysis of data was performed using Samtools and R Bioconductor packages.

Normalization and visualization: After aligning the control and Myg1 siRNA reads against the reference genome (as discussed above), the aligned reads were normalized. The normalization of control and MYG1 silenced sample was performed with respect to the control. The normalized control read counts were 1 for every co-ordinate (since they were divided by itself) and normalized read counts for MYG1 silenced sample were considered as fold change. For visualization purpose the normalized read counts for control and MYG1 silenced samples were plotted as two separate lines in the same plot (Figures 4-6; Blue line for control and red line for MYG1 silenced sample).

Supplementary Methods details other methods used in this study. This data is uploaded in ArrayExpress under the accession E-MTAB-7240.

RNA decay assay

B16 mouse melanoma cells were treated with Control and Myg1 siRNA. EU labeling, RNA isolation and RNA pull-down was done as per the protocol given by Chatterjee *et al.* (19). Detection of RNA was done by qPCR. Detailed protocol is provided in the supplementary methods.

Protein synthesis evaluation in B16 cells using Click-iT™ HPG Alexa Fluor™ 488 Protein Synthesis Assay Kit

Protein synthesis rate was evaluated by HPG incorporation in control and Myg1 knockdown B16 cells incubated with methionine free medium. The protocol for the same was followed as per manufacturer's instructions (Thermo #C10428).

Western blot analysis of mitochondrial proteins

B16 cells were transfected with Myg1 SiRNA using Dharmafect (SMARTpool:ON-TARGETplus Myg1 siRNA, L-055338-01-0005). After 24 h, the cells were trypsinized and lysed using NP40 lysis buffer supplemented with protease inhibitor cocktail. For detection of mitochondrial protein, 40 μg of cell lysate was resolved on 10% SDS-PAGE gel. Antibody was prepared in 2% skimmed milk solution with following dilutions MT-CO1(Abcam, ab90668, 1:500), MT-ND5(Abcam, ab92624, 1:500), MT-ATP6 (Abcam, ab192423, 1:100), MT-CYB(Abcam, ab81215, 1:100), Myg1 (Abcam, ab122493, 1:2000), Tubulin (Abcam, Ab21058, 1:5000). It was detected using HRP conjugated anti rabbit secondary antibody (1:10 000) and detected through Enhanced Chemiluminescence using ChemiDoc (Syngene).

RNA extraction and real-time PCR

Isolation of total RNA was performed using Nucleospin Triprep kit (MachereyNagel) according to manufacturer's

protocol. Quantitative real-time PCR with reverse transcription (qRT-PCR) was performed on a Roche Light Cycler 480 II real-time cycler using the KAPA SYBR FAST qPCR Master Mix (KAPA Biosystems) to evaluate transcriptional regulations. Gene specific primers were obtained from Sigma Aldrich. The relative transcript levels of each target gene were normalized against GAPDH mRNA levels; quantification was performed using the comparative Ct method. Detailed protocol is provided in the supplementary methods.

Oxygraph Oroboros O2k for yeast cells

2×10^6 B16 cells in DMEM high glucose or 1 $O.D._{600\ nm}$ of mid log culture *Saccharomyces cerevisiae* cells in YPD/SD(-Ura) medium were used for the Oxygen measurements. The Oroboros O2k instrument (O2K FluoRespirometer, Oroboros Instruments) was calibrated using corresponding medium before measurements. The cells were then added to the Oxygraph chamber and oxygen concentration was monitored. Validation of knockdown was done using western blot method from an aliquot of cells. Slope was calculated after linear fit using GraphPad Prism software.

RESULTS

Evaluating dual localization proteins for mediating nuclear-mitochondrial cross-talk

Synchronizing the functions of nucleus and mitochondria is essential for cellular bioenergetics. It is increasingly recognized that several proteins are localized to both nucleus as well as mitochondria, which are likely candidates for mediating the inter-organellar communication. Hence, we set out to identify the functional categories of dual localized proteins. Towards this, we compiled the list of nuclear and mitochondrial proteins from The Human Protein Atlas (20). Of the 8527 nuclear and 1259 mitochondrial proteins, 567 proteins were localized to both nucleus and mitochondria based on antibody as well as mass spectrometric evidence for their dual localization (Supplementary Table S1). Gene-set enrichment analysis using DAVID suite identified pathways and processes mapped to these proteins (Figure 1A). Enriched processes belong to translational regulation in mitochondria, components of the mitochondrial ribosome and RNA processing. Enzymes involved in metabolism and DNA repair that are anticipated to be dually localized, had lesser representation. Suggesting that the dual targeted proteins are primarily regulating translation and RNA processing events in mitochondria, and we set out to identify the crucial mediator. Notably, out of the 567 dual targeting proteins, three were not assigned to any of the processes, and were uncharacterized.

Among them C12orf10 encoding a protein Myg1 (MelanocYte proliferation Gene 1) was earlier demonstrated to localize to both nucleus and mitochondria and the corresponding localization signals have also been identified (21). Altered expression of Myg1 is observed in response to mitochondrial DNA damage and in hypomorphic alleles of PGC1-β, the key regulator of mitochondrial biogenesis (22,23). Therefore this uncharacterized gene C12orf10 emerged as a potential candidate that could regulate mitochondrial functionality. Genetic knockouts in model organisms display fitness defect under stress conditions, suggesting a non-essential but important role for Myg1 (24,25). Genetic and expression level changes in Myg1 are reported in a complex skin disorder vitiligo (26). Therefore we embarked on our study to characterize this gene and identify its role in mitochondrial physiology.

Myg1 is a 3′-5′ exonuclease with RNA as its preferred substrate

Myg1 belongs to the DHH motif containing family of phosphoesterase. Sequence based prediction of Myg1 with known structures by Genthreader analysis demonstrated best similarity with RecJ, a phosphodiesterase involved in DNA repair (Supplementary Figure S1). Known members of phosphodiesterases are involved in the hydrolysis of nucleic acid substrates. As both nucleus and mitochondria harbour DNA, and rapid RNA dynamics is prevalent across these two organelles, one or both of these are likely to be the substrate of Myg1. To gain further insights, we modeled Myg1 based on the known structure of RecJ. The C-terminal region was modeled based on several other structures with high local sequence similarity using a hybrid modelling protocol (Figure 1B and C). Overall topology of Myg1 is comparable to the DHH family of phosphodiesterases involved in RNA and DNA metabolism. To identify the biochemical functions of Myg1, we cloned, expressed and purified human Myg1 protein from *Escherichia coli*. Biochemical assays were performed with purified Myg1 and 5′ end labelled nucleic acids; single stranded DNA, double stranded DNA and single stranded RNA, as well as single stranded RNA with interspersed Locked Nucleic Acid (LNA) modifications, to identify the substrates of this phosphoesterase. We observed that Myg1 exhibits a robust exonuclease activity on RNA and to a lesser extent on single stranded DNA, but does not appreciably cleave the double stranded DNA (Figure 1D–F). The polarity of the enzyme is 3′-5′ as a ladder is observed (Supplementary Figure S3A). The enzyme demonstrated activity in presence of Mg^{2+} and in the presence of Mn^{2+} no nuclease activity was detected (Supplementary Figure S3E). Further, the enzyme did not demonstrate any detectable endonuclease activity, as RNA substrate with LNA modifications interspersed with phosphodiester bonds was not cleaved by Myg1 (Supplementary Figure S3F).

Potential substrate-binding site is localized at the interphase and in proximity are the catalytic DHH and substrate binding residues (Figure 1C). Interestingly, the substrate-binding region of Myg1 harbors His (344) in place of Gln (311) as observed in orthologous position in RecJ. In an independent study researchers have observed that the RNA metabolizing members of this superfamily have a conserved Histidine in this region (27). Hence we speculated that this could be responsible for the substrate specificity and performed site directed mutagenesis to generate $Myg1_{H344Q}$. Biochemical activity indicated that this mutant protein completely lacked RNAse activity and gained single stranded DNAse activity (Figure 1G). Thereby establishing that the wild type protein is a bona fide RNA exonuclease and the observed DNAse activity is residual.

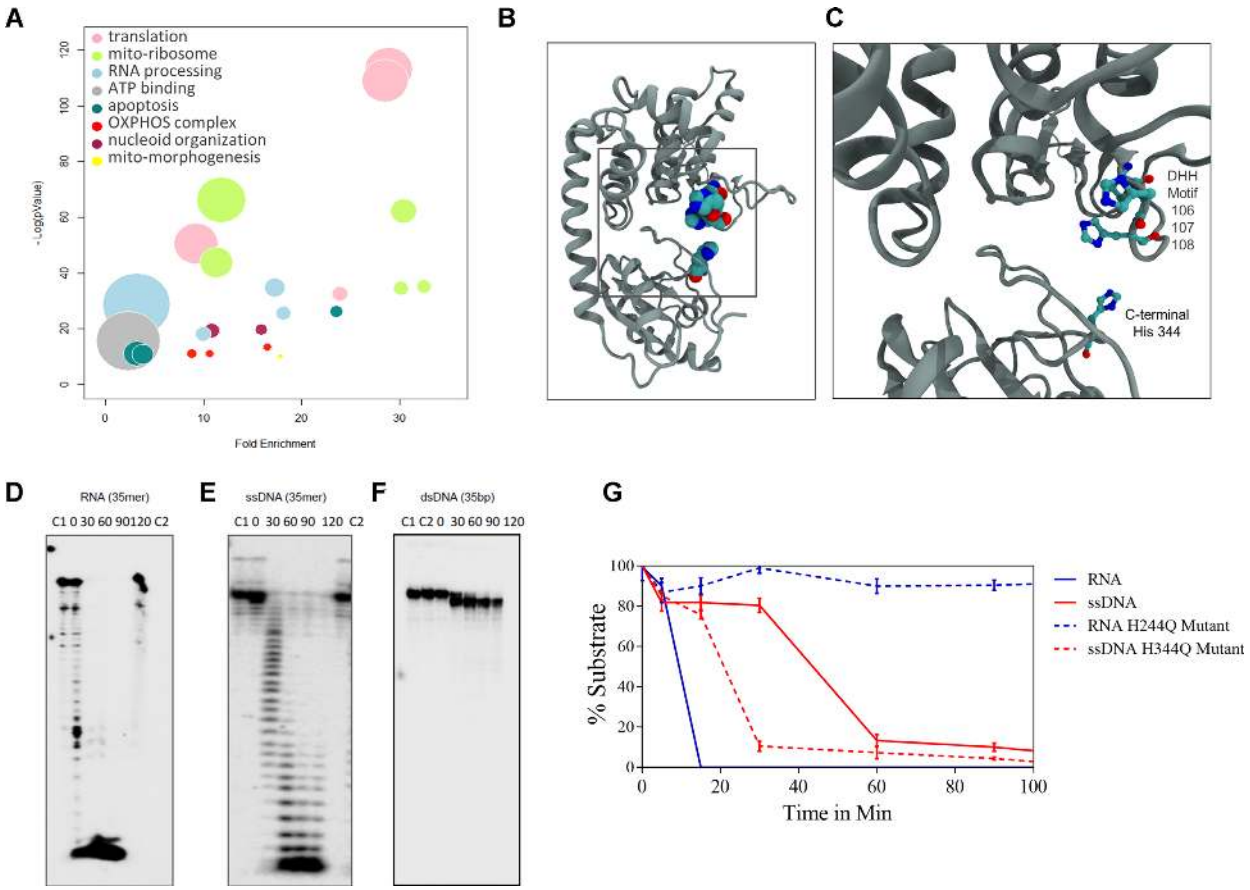

Figure 1. Myg1 is a dual localized protein with a 3′ to 5′ RNA exonuclease activity. (**A**) Bubble plot between the enrichment score and negative $\log_{10}$ of *P* value of enrichment by Gene Set Enrichment Analysis of dual localization proteins identified from The Human protein Atlas database. Size of the bubble indicates the number of genes. The Gene Ontology (GO) terms are colour-coded based on the overall category of the process involved. (**B**) Three dimensional structural model of Myg1 based on RecJ exonuclease (N-terminal) and the C-terminal region was modelled based on hybrid protocol using other templates with known structure. (**C**) Putative active site residues DHH (106–108) and conserved C-terminal Histidine 344 predicted to be involved in substrate selectivity are shown in the zoomed in image. In vitro exonuclease activity of wild type recombinant human Myg1 on (**D**) 35-mer RNA, (**E**) 35-mer single stranded DNA and (**F**) 35-mer double stranded DNA. All the substrates were 5′end-labeled with [γ-^{32}P] ATP and the activity was monitored at 0, 30, 60, 90, 120 min post addition of the enzyme. Lane C1 is a control reaction without the enzyme and lane C2 is a control reaction with heat-inactivated enzyme. (**G**) Kinetics of the exonuclease assays with wild type and mutant $Myg1_{H344Q}$ on 35-mer RNA and 35-mer single stranded DNA. Data represents the kinetic plot with mean values ± S.E.M. across two replicates.

Myg1 is a highly conserved gene and its knockout in yeast shows defects in respiratory growth

We set out to identify putative orthologs of Myg1 across organisms to unravel its cellular functions. The criteria to narrow down the aligned sequences were 45% query cover and presence of DHH motif responsible for catalysis in this family of phosphoesterases. Homologs with identity of around sixty per cent could be traced, covering all groups of organisms, indicating a conserved role for this gene (Figure 2A and Supplementary Table S1). However, the cellular functions of this RNA exonuclease remain elusive (28). To delineate the functions of Myg1 we chose *S. cerevisiae*, wherein knockout and complementation studies are feasible. Additionally, by changing the carbon source the yeast system enables switch from a fermentative to respiratory growth that necessitates mitochondrial functioning.

Spot assays with yeast knockout for Myg1 ortholog YER156c, displayed a growth defect in minimal medium and on the respiratory carbon source glycerol (Figure 2B, Supplementary Figure S5). As cells are required to utilize mitochondrial respiration based generation of ATP under glycerol as a carbon source, we speculated that the reduced growth on glycerol is indicative of mitochondrial defect. Mitotracker green staining of wild type and the *myg1Δ* strains indicated a reduction in mitochondrial mass (Supplementary Figure S5C). Since the primary role of mitochondria is oxidative phosphorylation (OXPHOS), we measured the oxygen consumption rate of wild type and Myg1 knockout yeast using Clark electrode. Oxygen consumption and levels of ATP were dramatically reduced in the knockout strain confirming loss of mitochondrial functionality (Figure 2C and D). Based on these results, it appears that Myg1 is an important factor required for the mitochondrial activity.

Complementation with the wild type human ortholog (hMYG1) that shares 63 per cent identity with the YER156c could rescue the growth defect of *myg1Δ* cells (Figure 2E), suggesting that despite vast differences in the evolutionary history, human counterpart can perform analogous functions in unicellular yeast. This observed rescue of growth

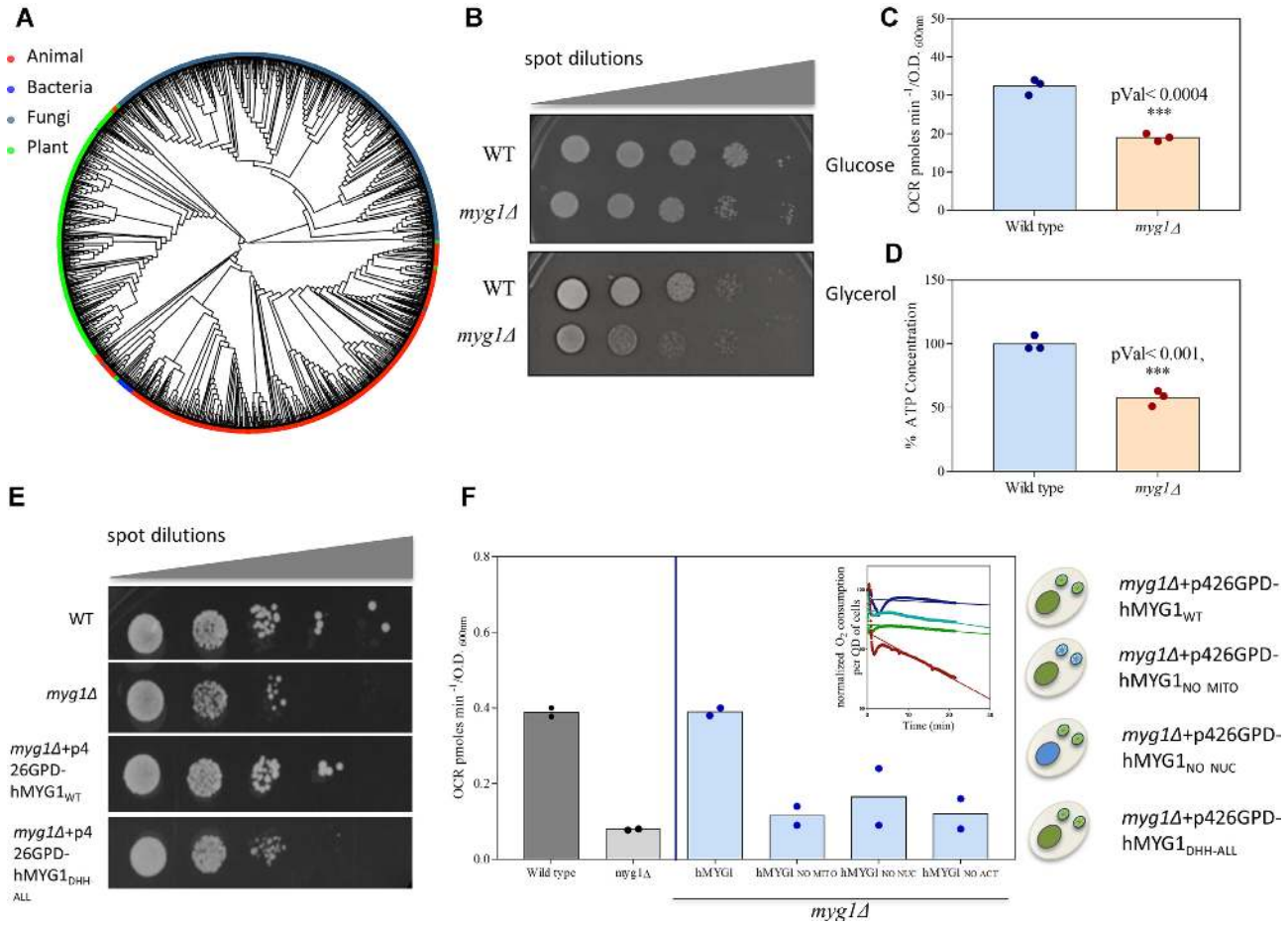

Figure 2. Myg1 is a highly conserved protein involved in mitochondrial functions. (**A**) Phylogenetic analysis of Myg1 homologs across various organisms with a minimum query cover of 45% and presence of DHH motif is depicted as a circular dendrogram. (**B**) Spot assays for the wild type and *myg1Δ* strains on fermentative medium containing yeast extract, peptone and dextrose (YPD) medium and respiratory growth medium containing yeast extract, peptone and glycerol (YPG) medium. Spot dilutions starting from 1 $O.D._{600\,nm}$ cells were ten-fold diluted across the plate. (**C**) The bar graph shows the mean and individual data points of oxygen flux in $pmol/min/OD_{600\,nm}$ cells as a representation of respiratory capacity measured by Oroboros O2k instrument in Wild type and *myg1Δ Saccharomyces cerevisiae* (BY4742) cells. The experiment was performed with 3 biological replicates. (Student's *t* test, $P < 0.0004$). (**D**) The levels of ATP was measured using luminescence based method in Wild type and *myg1Δ* strains across three replicates. The bar graph represents mean and individual data points in the ATP represented as a percentage of the wild type cells (Student's *t* test, $P < 0.001$). (E) Spot assay of wild type and *myg1Δ* strains upon complementation with human Myg1 (hMYG1) or the catalytically inactive DHH mutant Myg1 ($hMYG1_{DHH\text{-}ALL}$). (**F**) Bar graph depicts the oxygen consumption rate (OCR) as pmoles of oxygen consumed/min/ $O.D._{600\,nm}$ of *S. cereviasiae* culture across two independent biological replicates (mean ± SEM) in wild type yeast, *myg1Δ* strain. The same is depicted for complementations in the *myg1Δ* background with wild type human MYG1 targeting to both mitochondria and nucleus (hMYG1), nuclear targetting human Myg1 ($hMYG1_{No\ Mito}$), mitochondrial targeting hMYG1 ($hMYG1_{No\ Nuc}$) or the catalytically inactive mutant hMYG1 ($hMYG1_{DHH\text{-}ALL}$) complemented *myg1Δ* yeast cells. Inset represents kinetics of oxygen consumption in various yeast strains, their raw traces and linear fit in one representative experiment is depicted.

is dependent on the activity of Myg1, as catalytically inactive mutant ($Myg1_{DHH\text{-}ALL}$) despite expressing to comparable levels, failed to complement the growth. We therefore conclude that Myg1 is likely to govern mitochondrial functions and hence set out to identify its role.

Dual localization of Myg1 to both nucleus and mitochondria is necessary for cellular respiration

Earlier study has identified the localization signals in human Myg1 (hMYG1) to both nucleus and mitochondria (21). We generated mutants of hMYG1 that localize only to the nucleus or to mitochondria and tested for their ability to restore cellular respiration in the *myg1Δ* strain. This system harnesses the strength of genetic knockouts in yeast along with conditional growth to assess Myg1 functionality. We established that these mutants localize to predicted compartments in yeast by fractionation and then assessed the mitochondrial function (Supplementary Figure S12). Measurement of oxygen consumption was chosen as the mitochondrial functionality criteria for assessing complementation of the yeast *myg1Δ* strain.

While the oxygen consumption of hMYG1 was restored to that of the wild type, the inactive mutant ($hMyg1_{DHH\text{-}ALL}$) failed to consume oxygen and the rate was comparable to the knockout strain (*myg1Δ*) (Figure 2F). Interestingly, neither the nuclear ($hMYG1_{NoMito}$) nor mitochondrial ($hMYG1_{NoNuc}$) localization mutants could restore the oxygen consumption, emphasizing the need for Myg1 to localize both to nucleus and mitochondria for OX-

PHOS activity. Hence we conclude that the two spatially distinct roles of Myg1 are inter-dependent and Myg1 needs to localize to both compartments for mitochondrial respiration. We then resorted to identify the molecular basis for Myg1 functions.

Myg1 is localized to nucleolus, nucleoplasm and mitochondrial matrix

To decipher the cellular functions of Myg1, we performed co-localization with RNA and DNA by pulse labeling with ethenyl uridine (EU) and ethenyl deoxyuridine (EdU) respectively. These experiments were carried out in B16 cells, as the melanocyte proliferation gene 1 (Myg1) is likely to have an important role in melanocytic cells. Distinct localization of Myg1 within the nucleus was observed and these signals co-localized with freshly synthesized RNA (Figure 3A), but not with DNA (Figure 3B). Earlier studies had reported localization of Myg1 to nucleus and mitochondria. Immunolocalization demonstrated presence of Myg1 predominantly in the nucleolus (21). However, we could not detect the presence of Myg1 in mitochondria by immunocytochemical assay. Therefore we resorted to sub-cellular fractionation.

Biochemical fractionation demonstrated Myg1 to be localized to nucleolus as well as in mitochondria. Presence of Myg1 in the nucleoplasm indicated that this protein could be in an exchangeable pool (Figure 3C). It is noteworthy that there are two forms of Myg1 and both could be silenced using siRNA (Supplementary Figure S6). However, only the slow migrating form of the protein is localized in the two compartments, whereas the lower band is enriched in the cytoplasmic fraction derived after fractionating the cells with nucleus and mitochondria. It is likely that there is an additional regulation of Myg1 through post-translational processing or modification, such as acetylation that could result in differential migration.

Within mitochondria, the RNA is present in the matrix; hence we further traced the sub-mitochondrial localization of Myg1. Towards this, we treated purified mitochondria with a mild detergent Triton-X-100 and disrupted the outer membrane using hypotonic lysis. We observed that Myg1 was retained in mitoplast in a manner similar to the known matrix targeted protein SOD2, confirming its localization to the mitochondrial matrix (Figure 3D). Hence, Myg1 appears to be involved in the processing of RNA in these two compartments, and we hypothesized that Myg1 could fine-tune the RNA dynamics and mediate spatio-temporal communication across nucleus and mitochondria.

Silexoseq analysis: a method to map the *in vivo* cleavage trail of RNA exonuclease

While, within the cells RNA exonucleases are likely to be involved in selective cleavage, deciphering the substrate specificity using *in vitro* assays is a challenge. Currently there are no reliable methods available to identify the *in-vivo* substrates of exonucleases. CLIP and CRAC methodology has been employed to identify the foot-print of an RNA binding protein on specific transcripts (29,30). However, these are not effective for RNAse enzymes as opposed to RNA binding proteins that stably bind RNA. We had attempted CRAC analysis for Myg1 and did not identify specific RNA enrichment presumably due to RNA degradation. PARE sequencing is an efficient methodology that involves silencing the specific endonucleases and deciphering their footprint by deepsequencing. To identify the endonuclease cleavage site normalized frequency of reads with the inspected position as the first base is mapped (2,10). Cleavage site shows as a peak, due to overabunadance of reads with that nucleotide as the first base. However this could not be applied to exonucleases that have a trail on the transcript. Hence we developed a next generation sequencing based approach to identify targets of specific exonucleases.

We employed a total RNA sequencing method, using high coverage sequencing of RNA isolated from specific organelles to enrich low abundant precursors. As exonucleases have very high turnover rates, capturing them with RNA *in vivo* is a challenge. Hence, in this *silexoseq* (*si*lencing *exo*nuclease and RNA *seq*uencing) analysis, we adopted a silencing approach to compare the read coverage. A plot of normalized read coverage at every base position across the transcript would therefore be visible as a peak in region of the transcript processed by the exonuclease. Thus, the cleavage trail of that particular exonuclease could be mapped (Figure 4A).

We performed *silexoseq* of nuclear and mitochondrial compartments of B16 cells under Myg1 silenced state. As Myg1 localizes to the nucleolus, we speculated that it might have a role in ribosomal RNA processing that involves removal of internal and external transcribed regions. We mapped nuclear reads to rRNA locus and normalized coverage was analysed in 5′ETS (external transcribed spacer), 3′ETS as well as internal transcribed sequences ITS-1 and ITS-2. Reads at 5′ETS did not show any discernible pattern of accumulation and hence we concluded that they are not different (Supplementary Figure S7A). The mapped reads for the 3′ETS region in both control and silenced states were minimal, concordant with the notion of rapid degradation of this sequence (Supplementary Figure S7B). However, analysis of ITS-1 region revealed accumulation of reads, indicating the cleavage of ITS-1 by Myg1 (Figure 4B). While the majority of ITS-2 region does not show a peak, the 3′end has a short stretch where reads accumulate and could be an additional footprint of this enzyme (Figure 4C). This data suggests a role for Myg1 in rRNA processing and highlights the power of silexoseq analysis to identify in vivo substrates. Hence we further went ahead to validate this methodology using an orthogonal technique.

Validation of silexosequencing confirms that Myg1 processes ITS-1 region of ribosomal RNA

Processing of ribosomal RNA is fairly well understood and involves exonucleolytic and endonucleolytic processing events. Abundance of rRNA and its precursors along with the established processing that is already delineated allowed us to validate silexoseq analysis using northern blot. The eukaryotic nuclear rRNA is transcribed and processed in nucleolus and the assembly of ribosomes continues through the cytoplasm. This involves extensive processing of the multi RNA transcript to the 18S, 28S and 5.8S rRNAs that

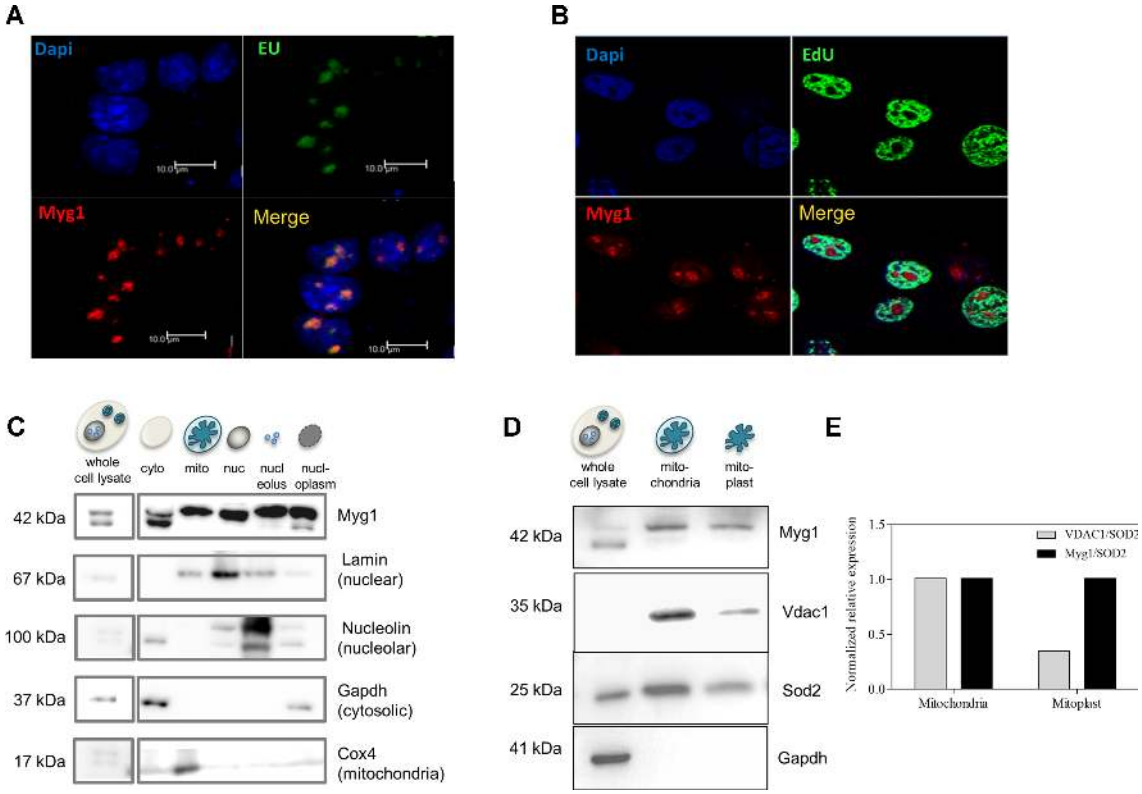

Figure 3. Myg1 localizes to nucleolus and mitochondrial matrix. (**A**) Myg1 co-localization with newly synthesized RNA stained with 5-ethynyl uridine (EU) (top right) in live B16 cells, later fixed and immunostained with Myg1 (bottom left) and the nuclear DNA is counter stained with DAPI (top left). RGB images of the maximal intensity projection of confocal sections of the nuclei are split into green, red and blue channels that reflect EU, Myg1 and DAPI staining respectively. Scale bar 10 μm. (**B**) Live B16 cells pulse chased with EdU (5-deoxyethynyl uridine), later fixed and immunostained with Myg1. RGB images of the maximal projection of the confocal sections of the nuclei are split into green, red and blue channels that reflect EdU, Myg1 and DAPI staining respectively. (**C**) Fractionation of B16 cells followed by detection of Myg1 by western blot analysis in nucleolus and mitochondria. Enrichment of fractions is ascertained by using antibodies to lamin (nuclear marker), GAPDH (cytosolic marker), nucleolin (nucleolar marker), Cox4 (mitochondrial marker) along with Myg1. (**D**) Mitochondria isolation and mitoplast preparation subjected to western blot analysis of VDAC1 present in mitochondrial outer membrane, SOD2 localizing to mitochondrial matrix along with Myg1. GAPDH was used to ascertain cytoplasmic contamination. (**E**) Relative intensity ratios of VDAC1 and Myg1 with respect to SOD2 in mitoplast is normalized to their relative ratio in mitochondria.

assemble into the mature 80S ribosome. Northern blot analysis carried out with probes mapping to internal transcribed spacers (ITS) 1 and 2 regions of mouse rRNA revealed accumulation of 41S as well as the 20S rRNA species (Figure 4D). Based on the known pattern of mammalian rRNA maturation (Figure 4E), this analysis confirmed the involvement of Myg1 in processing of ITS-1 region of rRNA, which is common to both 41S and 20S rRNA species that are accumulated upon Myg1 silencing. This validated the application of silexoseq analysis to identify *in vivo* targets.

Myg1 functions in ribosome maturation and promotes translation

Involvement of Myg1 in ITS-1 processing suggests that this exonuclease could modulate the ribosomal assembly and maturation that take place simultaneously. To address the localization of Myg1 on pre-ribosomal assembly complexes, we fractionated the cellular contents on a sucrose density gradient followed by the detection of Myg1 by western blot analysis. The fractions were monitored for ribosomal proteins and the RNA content to ascertain the identity of fractions. Myg1 co-fractionated with 40S ribosomal subunits but not with 60S, 80S or the polysomal fractions, indicating a role in assembly of pre-40S complex (Figure 4F). In this context, it is interesting to note that the yeast knockout for Myg1 had lower 40S and 80S peaks. But the 60S peak was comparable, suggesting a conserved role for Myg1 in ribosome maturation and alterations in its functions could lead to translational changes in the cell (Supplementary Figure S8A).

To determine whether these changes in ribosomal RNA cleavage and consequent changes in ribosome result in protein synthesis alterations, we performed pulse-labeling experiments with B16 cells using ^{35}S-methionine (Supplementary Figure S8B). Independently, labeling of cells using a methionine analogue L-homopropargyl-glycine (HPG) and detection using click chemistry based fluorophore conjugation, validated a decrease in protein synthesis rate. A delay in the incorporation of label upon Myg1 silencing confirmed decreased ribosomal functionality. Thereby we demonstrate that Myg1 is involved in processing the ribosomal RNA and governs the translational capacity of the cell.

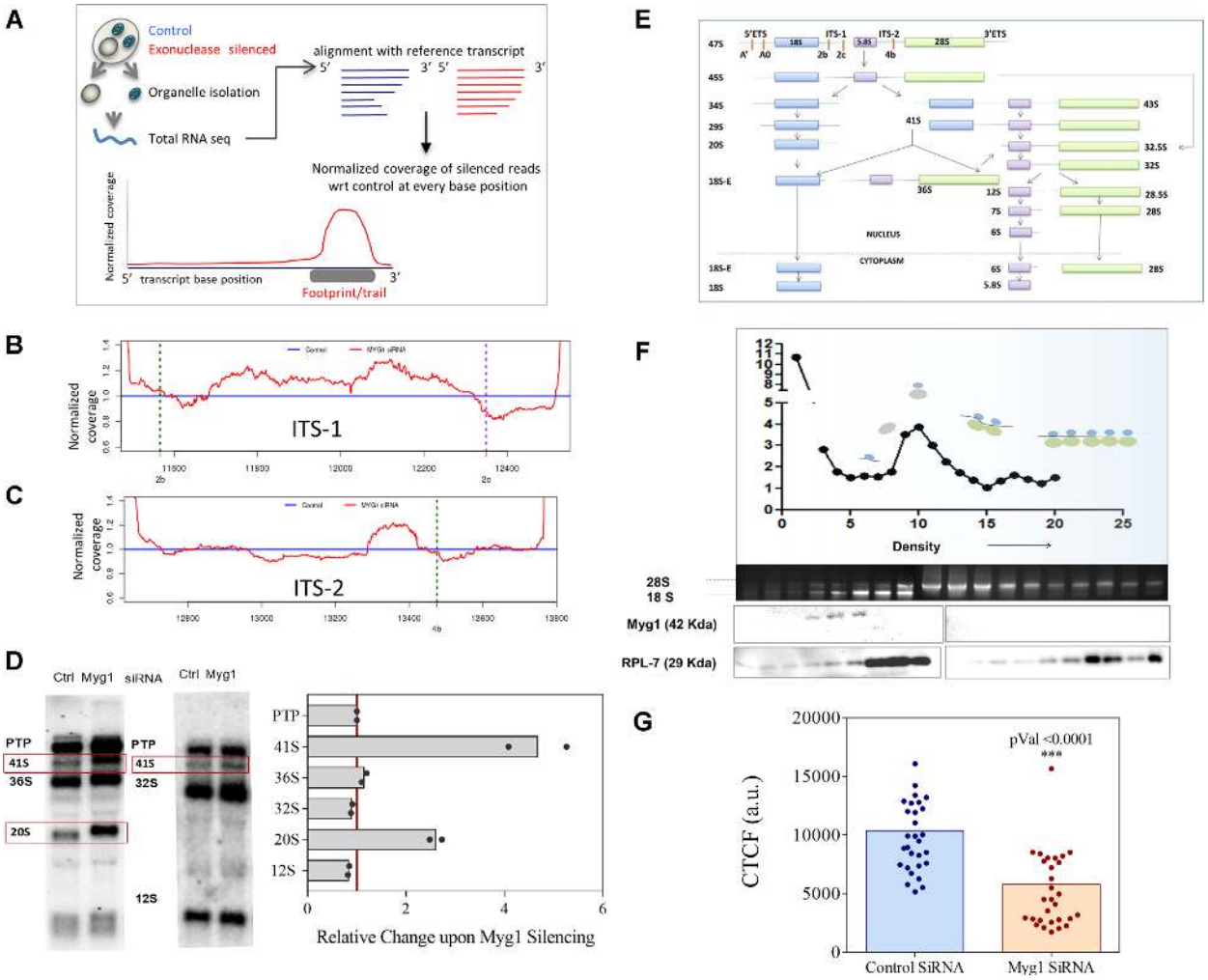

Figure 4. Establishment of Silexoseq analysis and involvement of Myg1 in ribosomal RNA processing. (**A**) Schematic representation of the anticipated pattern of the read accumulation in Silexoseq (silencing of exonuclease and sequencing) analysis of a 3′-5′ exonuclease. The red lines indicate the pattern of transcripts upon silencing and in blue are the control pattern with an active 3′-5′ exonuclease. Upon normalizing the sequencing read counts at every base position, a peak would be observed in regions where exonuclease cleaves the transcript. Silexoseq analysis of (**B**) ITS-1, (**C**) ITS-2 regions of the ribosomal RNA upon Myg1 knockdown. (**D**) Northern blot analysis of control and Myg1 silenced B16 cells using probes that map to ITS-1 and ITS-2 regions. (**E**) The hybridization signal from 47S, 46S and 45S pre-rRNA is labeled as the 'primary transcript plus' (PTP) and 41S, 36S, 32S, 20S and 12S are represented as relative change with respect to control cells. Bars represent mean and individual data points across two replicates. (**F**) Fractionation of cycloheximide treated B16 cells on linear 10–50% sucrose gradient analysed for the rRNA followed by western blot analysis for Myg1 and RPL7. (**G**) Bar plot for the cell translation analysis performed by Click iT™ HPG Protein synthesis kit in B16 cells treated with Control and Myg1 siRNA. The scatter plot from three independent experiments (unpaired Student's *t* test, $P < 0.0001$).

Myg1 cleaves nuclear encoded mitochondrial (NeMito) transcripts

To understand the nuclear role of Myg1 in detail, we performed RNA-seq analysis from purified nuclei in both control and Myg1 knockdown B16 cells and analysed changes in the expression of transcripts as fold change in FPKM values. We observed a total of around 775 upregulated genes and 592 downregulated genes with a fold change 2 in the nuclear compartment (Supplementary Figure S9). Gene Set Enrichment Analysis (GSEA) of upregulated genes using DAVID suite revealed several processes to be altered (Figure 5A, Supplementary Table S2). Top most process with highest enrichment score and lowest *P* value pertains to mitochondrial functions. The other set of enriched processes includes ribosomal machinery and regulators of translation, which is synergistic with its role in ITS-1 processing leading to ribosome maturation. We hypothesized that Myg1 could be responsible for altering these two central cellular processes. Upon further investigation, many of the nuclear encoded mitochondrial (NeMito) genes encoding electron transport chain and mitoribosomes were found to be upregulated (Figure 5B). We validated the enrichment of these transcripts upon Myg1 silencing by q-RT PCR (Figure 5C).

Silexoseq analysis was performed to check whether the abundance is because of 3′ end processing by Myg1. NeMito mRNAs NDUFB7 and NDUFB11 that are abundant in the nucleus when subjected to the analysis indicated a trail at the 3′ end strengthening the possibility of direct cleavage by Myg1 (Figure 5D and E). It is likely that the increase in

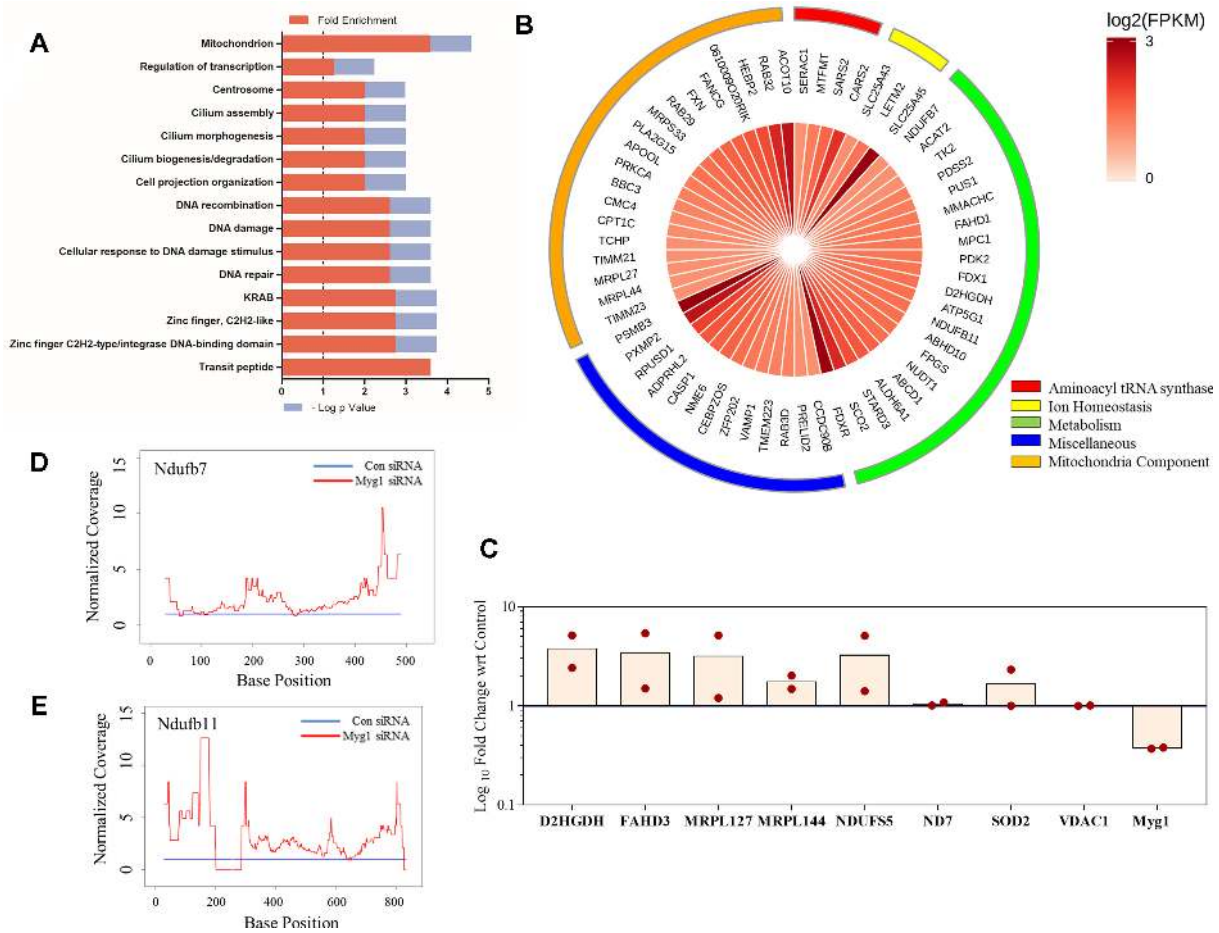

Figure 5. Myg1 cleaves NeMito transcripts. (**A**) Pathway enrichment analysis performed on the set of upregulated genes (fold change > 2) in Myg1 siRNA treated B16 cells. Negative logarithm of enrichment *P* value and the fold enrichment score; outputs from DAVID gene set enrichment analysis are plotted for processes with *P* value $< 10^{-7}$. (**B**) Heatmap for the list of nuclear encoded mitochondrial genes (NeMito) that are upregulated in the enrichment analysis. Colour code outside the Heatmap represents specific process within the mitochondria. (**C**) Real time PCR analysis of NeMito Genes in B16 cells upon Myg1 silencing. The experiment was performed in 2 independent biological replicates and the data represented is the mean and individual data point. (**D**, **E**) Silexoseq analysis of abundantly expressed NeMito RNAs Ndufb7 and Ndufb11.

nuclear encoded mitochondrial (NeMito) transcripts could be due to direct cleavage by Myg1. It is interesting to note that NeMito genes are also transcriptionally co-regulated by a common transcription factor GPS2 (31). Myg1 provides additional layer of regulating these set of genes that are encoded in the nucleus but have a function in mitochondria.

Ribosomal and messenger RNA transcripts in mitochondria are targets of Myg1

Silexoseq analysis for the mitochondrial compartment was carried out. The plot in Figure 6A maps various genes encoded by the mitochondrial genome and displays the silexoseq peaks mapped to various genes. Several cleavage trails of Myg1 could be observed on the heavy transcript (Figure 6A). Interestingly these trails were sharp, distinct and restricted to ends of genes that are color coded at the backdrop. The peaks were clearly distinguishable from the baseline fluctuations. On a closer analysis these footprints mapped to the 3′end of the mature mRNA and rRNAs which is in tune with the 3′-5′ exonuclease activity of Myg1 (Supplementary Figure S11). However we did not observe Myg1 trail in any of the tRNAs encoded by the heavy strand. Overlapping genes that are a part of the same transcript such as ND4L/ND4 and ATP8/ATP6 do not have an intervening *silexoseq* peak, indicating that the mature RNA with a free 3′ ends are recognized and cleaved (Supplementary Table S3, and Supplementary Figure S11).

The mitochondrial genome is transcribed bidirectionally leading to the heavy and light transcripts. While most of the genes are encoded by the heavy strand a few of the genes arise from the light strand. Cognate regions in the more abundant heavy transcript needs to be cleared by degradation. We observe a strong silexopeak peak in tRNA-Ser^{UCN} that maps to 5′ end of the gene. We speculate that this peak could be the cleavage trail of the complementary heavy strand that requires degradation. Notably the tallest peak in heavy transcript maps to the 3′ end of the 12S rRNA and another sharp peak was observed at the 3′ end of 16S rRNA. Based on these footprints, we conclude that Myg1 is involved in exonucleolytic cleavege of mitochondrial ribosomal and messenger RNAs.

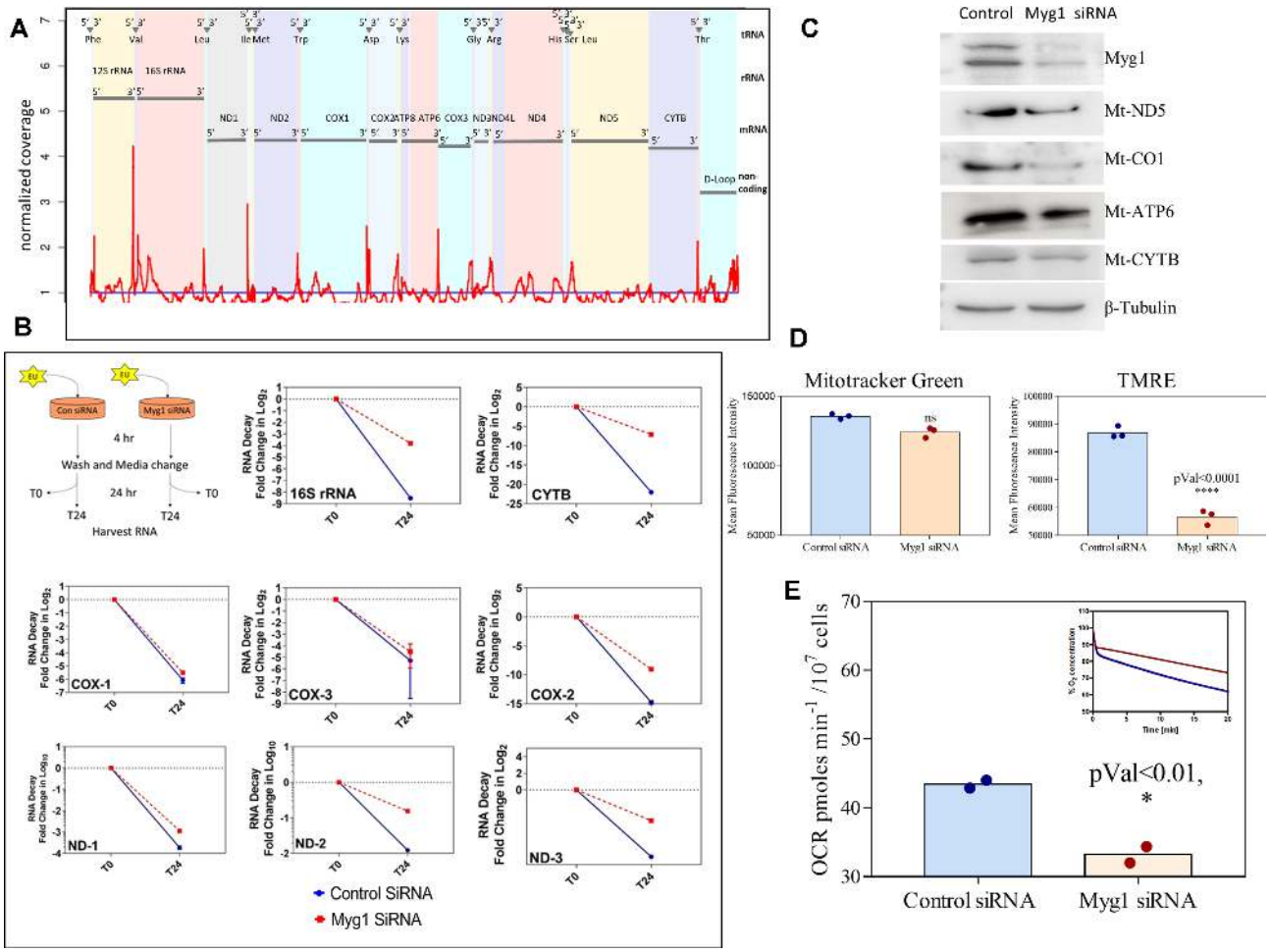

Figure 6. Myg1 mediates selective RNA turnover in mitochondria and governs OXPHOS. (**A**) Silexoseq analysis of isolated mitochondria from control and Myg1 silenced cells was carried out. Representation of the heavy strand of mitochondria; coordinates in the x-axis represent the genomic coordinates (in 5′ to 3′ direction) in continuum and each of the genes are highlighted in different colors at the backdrop. (**B**) RNA decay analysis performed by EU labeling in B16 cells treated with control and Myg1 siRNA. (**C**) Western blot analysis of ND5, CO1, ATP6, CYTB along with Myg1 from the whole cell lysates of B16 cells normalized to tubulin levels in control and Myg1 silenced cells. (**D**) Flow cytometric analysis of B16 mouse melanoma cells treated with Control and Myg1 siRNA and stained with TMRE to check the mitochondrial potential and MitoTracker green to check the mitochondrial mass. Experiments were performed with three independent biological replicates and represented as mean and individual data points (students t test for mitotracker green staining means not significantly different, and for TMRE staining P value < 0.0001). (**E**) Oxygen consumption measured using Clark Electrode in control and Myg1 siRNA treated B16 mouse melanoma cells. The traces correspond to the level of oxygen at various time intervals after addition of cells to the Oroboros chamber normalized to the level of oxygen at the time of addition of cells (inset). Oxygen consumption rate (OCR) determined from the slope of the curve is depicted as pmoles of oxygen consumed per minute per 10^7 of cells, calculated from two independent biological replicates with comparable Myg1 silencing represented as mean and individual data points (Student's t test, $P < 0.01$).

It is noteworthy that Myg1 processes ITS-1 region and helps in the maturation of 18S rRNA for the assembly of cytoplasmic ribosomes. However, given the thrifty genome and absence of any ITS and ETS regions in the mitoribosomal RNA, it is difficult to assign a processing role for this exonuclease in mitochondria. Heterogeneity and poly/oligo adenylation of mammalian ribosomal RNA has been observed and is suggestive of high rate of turnover of the RNA species (32). Based on the selective footprint of Myg1 in the 3′ ends of mRNA and rRNAs we speculated its involvement in the turnover of mitochondrial RNA.

Based on these observations absence of Myg1 functions would result in the accumulation of these transcripts. Therefore we studied the RNA decay kinetics upon Myg1 silencing. This involved pulse labelling of RNA using EU, followed by RNA isolation and conjugation of biotin at the end of labelling and after a 24h chase period. Following the pull down of labelled RNA using streptavidin, individual transcripts were quantified by qRT PCR. Decay kinetics indicated that upon silencing of Myg1 most of the mRNAs as well as 16s rRNA showed a reduced degradation kinetics (Figure 6B). Hence our study establishes that Myg1 plays an important role in RNA turnover in mitochondria.

Myg1 is required for mitochondrial functionality

Given the centrality of RNA dynamics, it is intuitive that Myg1 would govern mitochondrial functions. Alterations in mitoribosomal and messenger RNAs would be reflected in the steady state levels of mitochondria-encoded proteins. We observed that Myg1 silencing decreases several of these

proteins that are translated in the matrix (Figure 6C). This decrease is not due to the alterations in number of mitochondria, as mitotracker green staining demonstrated comparable levels (Figure 6D). Whereas, the mitochondrial potential measured by the Tetramethyl Rhodamine ethyl ester (TMRE) staining confirmed a dramatic reduction in the mitochondrial potential (Figure 6D). Upon further investigation of the mitochondrial functions, we observed that the oxygen consumption rate of the control siRNA cells was 42.9 ± 0.6 pmol of O_2 consumed/s/million cells. Whereas, upon Myg1 silencing this decreased to 34.4 ± 1.35, indicating a reduction in oxidative phosphorylation. Together these results point out that Myg1 is involved in mitochondrial RNA processing and governs mitochondrial functions.

RNA processing and mitochondrial alterations mediated by Myg1, is evident in the complex disorder vitiligo

Complex disorders often have multiple alterations that lead to the final disease manifestation. In an attempt to identify the molecular basis of a complex disease we have studied vitiligo, wherein genetic associations as well as expression level changes in Myg1 have been implicated across several populations (26,33). This localized depigmenting disorder permits comparison of the matched affected and unaffected skin. By this strategy, elevated ROS levels, as well as higher cellular response to the oxidative stress is observed in vitiligo lesions (34–36). Global transcriptome analysis revealed concordant changes that are likely to support the maintenance of depigmented lesions in vitiligo (37).

We first confirmed decrease in the expression of Myg1 in vitiligo lesions and observed that 13 out of 15 subjects showed a considerable downregulation in the average Myg1 signal in microarray (Figure 7A). Further, a detailed analysis of the upregulated genes was carried out. We selected the upregulated set of genes based on fold change of 2-fold or above as well as concordance across all the 15 pairs tissues (paired t test P value $< 10^{-7}$). Gene Set Enrichment Analysis of this set highlighted RNA processing and mitochondria related processes to be enriched (Figure 7B). Among the set of upregulated genes, ten of the 786 genes are also upregulated in B16 melanocytes upon Myg1 silencing, as depicted in the heat map in (Figure 7C). These genes belong to ribosomal components (RPS27A, RPL31 and RPL26), OXPHOS (NDUFS5) and mitoribosomal subunit protein (MRPS33). On further analysis of these three processes in the vitiligo microarray we observed several other genes belonging to ribosomes, mitoribosomes and OXPHOS to be significantly upregulated in the lesional skin (Figure 7D). We propose that Myg1 could explain the mitochondrial involvement reported in vitiligo at least in part. Thereby, offering a tantalizing opportunity to investigate targeting of Myg1 in this complex disorder. In effect we characterize a hitherto unknown protein Myg1 and establish the central role played by this protein in controlling mitochondrial functions in healthy and diseased states.

DISCUSSION

In this study we have identified a novel RNA exonuclease as a key orchestrator of mitochondrial functions. We establish that Myg1 has a 3′ to 5′ RNA exonuclease activity by biochemical assays. Further, by developing a methodology to map the cleavage trail of specific exonuclease, we determine the identity of preferred cellular substrates along with the trail of this enzyme on specific transcripts. Using these approaches, we discover three functions of Myg1 viz., maturation of 18S rRNA by the cleavage of ITS-1 region, cleavage of NeMito mRNAs in the nucleus and RNA turnover in mitochondria.

As current methodologies do not permit capturing RNase along with the RNA substrate, presumably due to high catalytic rate of these enzymes, silexoseq was necessitated to identify specific transcript substrates *in vivo*. PARE sequencing methodology excellently captures the cleavage sites for endonucleases. However, identification of the trail for exonucleases is complicated, as the cleaved nucleotides do not contribute to the sequencing reads. Therefore, we adopted a silencing based approach to map the cleavage trail and analysed differential accumulation of reads at every nucleotide position. By combining this strategy with organelle specific RNA isolation, we could enhance the read coverage of less abundant precursors, in addition to eliminating mitochondrial pseudogenes encoded by the nucleus. Our approach would complement methods such as PARE sequencing and MitoString analysis to identify and establish novel players in RNA metabolism (2,18).

Enrichment of reads at the 3′ end in silexoseq analysis is indicative of direct cleavage by Myg1, which demonstrates a 3′-5′ RNA exonuclease activity *in vitro*. Conservation of sequences in the trail or region upstream to it would provide clues to the sequence selectivity of this exonuclease, however we did not observe common consensus sequence or structural motifs (Supplementary Figure S14). Based on the varied propensity of targets to form stem loop structures, we speculate that the choice of *in vivo* substrates could be dictated by cellular factors such as RNA granule formation (9).

The first function of Myg1 emerged from its localization to nucleolus, the primary site involved in processing and assembly of ribosomes. By employing silexoseq analysis we arrived at the role of Myg1 in processing ITS-1 region that was substantiated by northern blot analysis. The knockout of Myg1 in yeast results in alterations in ribosome assembly, confirming a conserved role. Based on these observations we propose Myg1 to be a crucial exonuclease involved in rRNA processing that modulates ribosome assembly. Previous studies have shown an exosome component EXOSC10/Rrp6, to be involved in 3′ end maturation of 18S rRNA in human cells (11). It is therefore likely that Myg1 functions as an alternate exonuclease in ITS-1 processing and the process could be differentially regulated in a cell type or context dependent manner.

The second function of Myg1 is in processing the NeMito transcripts in nucleus. Around 12% of the upregulated genes in nucleus upon Myg1 silencing feature in Mitocarta database (38). The NeMito genes are critical components of the mitochondria and their processing by Myg1 offers a direct regulation of mitochondria by the nucleus. The concept of specialized ribosomes dedicated to translate NeMito proteins is being increasingly debated (39,40). Given the role of Myg1 in processing ITS-1 region, it is tempting to speculate

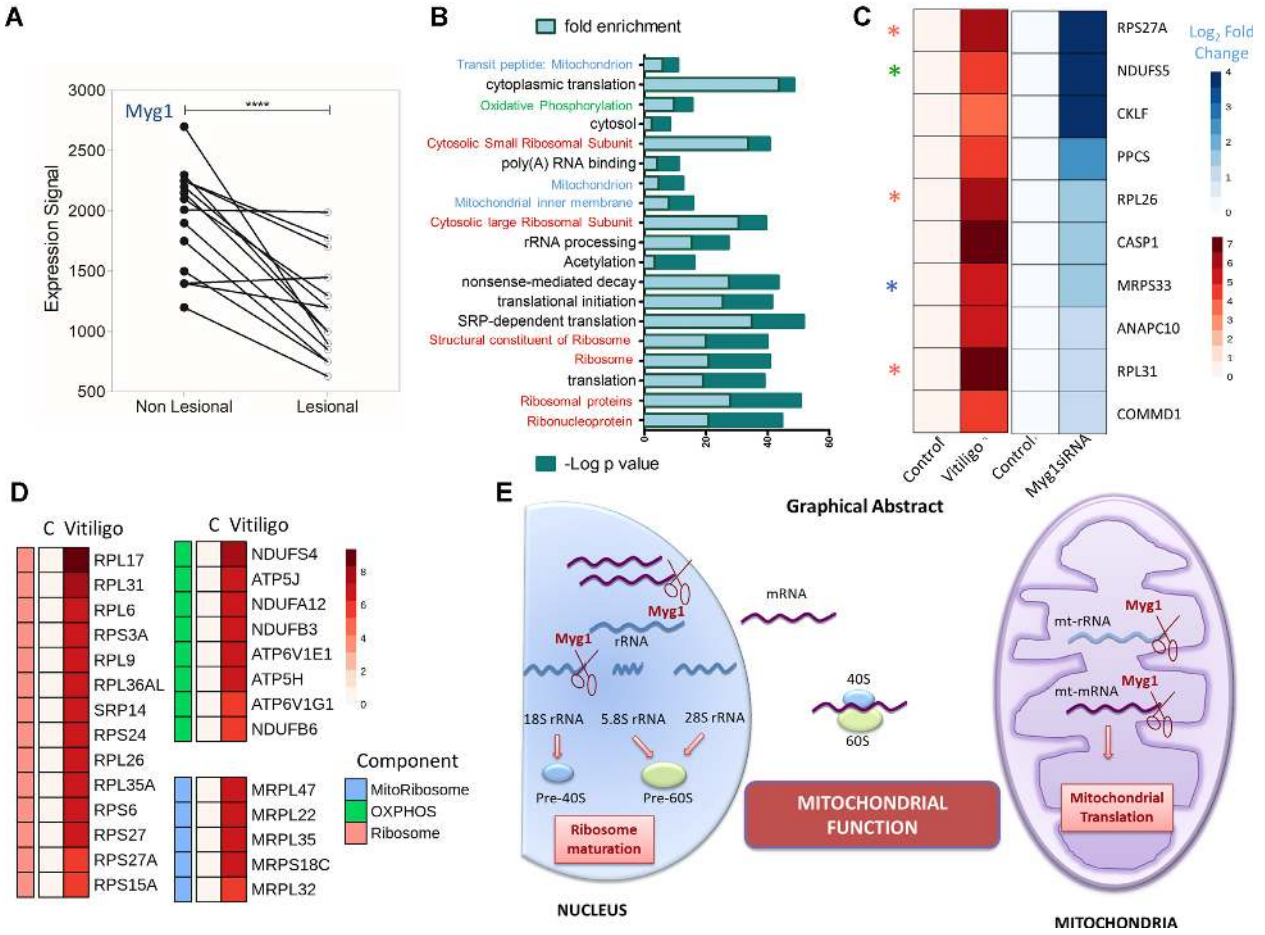

Figure 7. Footprint of Myg1 is evident in the complex disorder vitiligo. (**A**) Expression signals for Myg1, across non-lesional and lesional epidermis in the vitiligo microarray is depicted as a paired scatter plot (Student's paired *t* test, $P < 0.0001$). (**B**) Pathway enrichment analysis performed on the set of upregulated genes in microarray (fold change > 2 and *P* value $< 10^{-7}$) that compares lesional with the non-lesional epidermis of fifteen vitiligo subjects. Negative logarithm of enrichment *P* value and the fold enrichment score, outputs from DAVID gene set enrichment analysis are plotted for processes with *P* value $< 10^{-7}$. (**C**) Heatmap of common genes upregulated between Myg1 silenced B16 cells and vitiligo microarray. Asterix are colour coded to map genes to processes elaborated in D. (**D**) Heatmap of mitoribosomes, OXPHOS and ribosome related genes that are upregulated in lesional compared to non-lesional vitiligo skin. (**E**) Schematic depiction of the dual role of Myg1 in nucleus and mitochondria.

that these two nuclear roles of Myg1 could control mitochondrial functions in synchrony.

The third function of Myg1 is pruning of mitochondria encoded RNAs and is likely to be a direct way to control mitochondrial functions. Processing of the polygenic message by Myg1 came as a surprise as the trail maps to important coding regions of the mature rRNA as well as some mRNAs. RNA species including 16S and 12S rRNAs are known to be poly/oligo adenylated in a non-templated manner at their 3′ end, which is associated with their stability (32,41). In the mitochondrial matrix, susceptibility of RNA to oxidative damage is likely, necessitating RNA turnover (42). Hence degradation of mitochondrial RNA is imminent but the repertoire of involved components in mammalian system are not known. Recently, EXD2, an exonuclease that recognizes and cleaves several kinds of nucleic acid substrates in the mitochondrial matrix was shown to be important for translational fidelity (16). It is likely that Myg1 could work with other such exonucleases to achieve RNA homeostasis in mitochondria. Based on the observed trail and an accompanying reduction in the steady state levels of mitochondrial OXPHOS components, we conclude that Myg1 is a crucial player in mitochondrial remodelling achieved by the dual localization of this protein.

Upon Myg1 silencing, the set of upregulated nuclear mRNAs show enrichment of mitochondrial genes that are key constituents of complexes I, II, IV and V, as well as the mitoribosomal proteins. This accumulation is likely to arise from direct processing of nuclear encoded mitochondrial (NeMito) transcripts by Myg1. Recent studies have identified GPS2 as a transcriptional regulator in both mitochondria and nucleus. This protein governs expression of NeMito genes and facilitates mitochondrial biogenesis (31). Together with Myg1, the two form a tight regulatory network that governs mictochondrial functionality.

The three Myg1 controlled events appear to be interconnected and point to the mitochondrial regulation. Simultaneous synthesis and turnover of RNA ensures rapid regulation of the steady state levels that would be required during adaptations. The well-studied example of shift from a fer-

mentative to an oxidative metabolism involves rapid coupling of cytoplasmic and mitochondrial translation of OXPHOS complexes (8). Myg1 controls the cytoplasmic translatability of NeMito messenger RNAs. The mitochondrial message and mitoribosomal translation are governed by its matrix localization. Hence, Myg1 could orchestrate nucleo-mitochondrial coupling efficiently in a dynamic manner as per requirements of the cell.

During eukaryotic evolution that involves intra-cellular compartmentalization, coordinating the functionality of interdependent organelles such as nucleus and mitochondria would have been an important challenge to overcome. Incidentally, the closest homolog of Myg1 in bacteria shares a very high (almost 50%) identity with human Myg1 and belongs to PVC (Planctomycetes, Verrucomicrobia, Chlamydiae) class of bacterial super phylum that is thought to have paved the way for evolution of cellular compartmentalization (43). The sequence conservation of Myg1 as well as the ability of human Myg1 to complement the yeast knockout, highlights conserved nature of RNA metabolism. This could have led Myg1 to be a key player in harmonizing the mitochondrial endosymbiont with the central nuclear program.

Aberrant mitochondria affect disease progression by restricting cellular functions, which is being widely recognized in complex disorders but the underlying mechanisms remain unclear. Restoring mitochondrial functions thereby offers a tantalizing opportunity for clinical management in such disorders as well as conditions such as ageing. Several lines of evidence indicate involvement of mitochondria in vitiligo, a disorder with localized melanocyte loss, widespread tissue architecture and redox perturbations, that prevent melanocyte repopulation of chronic depigmented lesions (44–46). Based on our analysis it is evident that the interconnected networks of mitochondrial OXPHOS, mitochondrial translation as well as nucleo-cytoplasmic translation are altered in vitiligo, providing a molecular basis and credence to earlier observations (47). Genetic variations in Myg1 and its association with vitiligo are documented from Indian and Estonian populations. In this study we establish Myg1 as a key orchestrator of mitochondrial functions and provide molecular data that indicates a plausible role in the complex disorder vitiligo. Further investigations in this league to establish causality would pave the path for targeting this enzyme for future vitiligo therapies.

SUPPLEMENTARY DATA

Supplementary Data are available at NAR Online.

ACKNOWLEDGEMENTS

We acknowledge the infrastructural support of CSIR to the imaging facility (VISION-BSC0403). We would like to acknowledge constructive discussions regarding the work with Ankit Sabharwal, Kannan Boosi Narayanarao, Aarushi Singhal, Arpita Ghosh, Amrita Singh, Mohd Azhar and Vignesh Chandra Sekaran from CSIR-IGIB. Sangeeta Khanna is acknowledged for help with data analysis and representation. R.S.G. is a J.C. Bose Fellow of the Department of Science and Technology, Government of India (SB/S2/ JCB-038/2015).

FUNDING

Council for Scientific and Industrial Research [BSC0302]; Department of Biotechnology [GAP182]. Funding for open access charge: Department of Biotechnology.

Conflict of interest statement. R.S.G. is the co-founder of Vyome Biosciences Pvt. Ltd, a biopharmaceutical company in the area of dermatology unrelated to the work presented here. Other authors do not have any competing interests.

REFERENCES

1. Scarpulla,R.C., Vega,R.B. and Kelly,D.P. (2013) Transcriptional integration of mitochondrial biogenesis. *Trends Endocrinol. Metab.*, **23**, 459–466.
2. Mercer,T.R., Neph,S., Dinger,M.E., Crawford,J., Smith,M.A., Shearwood,A.J., Haugen,E., Bracken,C.P., Rackham,O., Stamatoyannopoulos,J.A. *et al.* (2011) Resource the human mitochondrial transcriptome. *Cell*, **146**, 645–658.
3. Rouquette,J. and Gleizes,P. (2005) Nuclear export and cytoplasmic processing of precursors to the 40S ribosomal subunits in mammalian cells. *EMBO J.*, **24**, 2862–2872.
4. Silva,D. De, Tu,Y., Amunts,A., Fontanesi,F. and Barrientos,A. (2015) Mitochondrial ribosome assembly in health and disease. *Cell Cycle*, **14**, 2226–2250.
5. Olson,M.O.J. and Dundr,M. (2000) The nucleolus: an old factory with unexpected capabilities. *Trends Cell Biol.*, **10**, 189–196.
6. Houseley,J. and Tollervey,D. (2009) Review the many pathways of RNA degradation. *Cell*, **136**, 763–776.
7. Small,I.D., Rackham,O. and Filipovska,A. (2013) Organelle transcriptomes: products of a deconstructed genome. *Curr. Opin. Microbiol.*, **16**, 652–658.
8. Couvillion,M.T., Soto,I.C., Shipkovenska,G. and Churchman,L.S. (2016) Synchronized mitochondrial and cytosolic translation programs. *Nature*, **533**, 499–503.
9. Jourdain,A.A., Boehm,E., Maundrell,K. and Martinou,J.C. (2016) Mitochondrial RNA granules : Compartmentalizing mitochondrial gene expression. *J. Cell Biol.*, **212**, 611–614.
10. Liu,G., Mercer,T.R., Shearwood,A.J., Siira,S.J., Hibbs,M.E., Mattick,J.S., Rackham,O. and Filipovska,A. (2013) Resource mapping of mitochondrial RNA-Protein interactions by digital RNase footprinting. *Cell Rep.*, **5**, 839–848.
11. Tafforeau,L., Zorbas,C., Langhendries,J., Mullineux,S., Stamatopoulou,V., Mullier,R., Wacheul,L. and Lafontaine,D.L.J. (2013) Resource the complexity of human ribosome biogenesis revealed by systematic nucleolar screening of Pre-rRNA processing factors. *Mol. Cell*, **51**, 539–551.
12. Bogenhagen,D.F., Martin,D.W. and Koller,A. (2014) Initial steps in RNA processing and ribosome assembly occur at mitochondrial DNA nucleoids. *Cell Metab.*, **19**, 618–629.
13. Reinhard,L., Sridhara,S. and Martin,B.H. (2018) The MRPP1 / MRPP2 complex is a tRNA-maturation platform in human mitochondria. *Nucleic Acids Res.*, **45**, 12469–12480.
14. Wang,G., Chen,H., Oktay,Y., Zhang,J., Allen,E.L., Smith,G.M., Fan,K.C., Hong,J.S., French,S.W., Mccaffery,J.M. *et al.* (2010) PNPASE regulates RNA import into mitochondria. *Cell*, **142**, 456–467.
15. Liu,X., Fu,R., Pan,Y., Meza-sosa,K.F., Zhang,Z., Liu,X., Fu,R., Pan,Y., Meza-sosa,K.F., Zhang,Z. *et al.* (2018) PNPT1 release from mitochondria during apoptosis article PNPT1 release from mitochondria during apoptosis triggers decay of poly (A) RNAs. *Cell*, **174**, 187–195.
16. Silva,J., Aivio,S., Knobel,P.A., Bailey,L.J., Casali,A., Vinaixa,M., Garcia-cao,I., Coyaud,É., Jourdain,A.A., Pérez-ferreros,P. *et al.* (2018) EXD2 governs germ stem cell homeostasis and lifespan by promoting mitoribosome integrity and translation. *Nat. Cell Biol.*, **20**, 162–174.

17. Rorbach,J., Nicholls,T.J.J. and Minczuk,M. (2018) PDE12 removes mitochondrial RNA poly (A) tails and controls translation in human mitochondria. *Nucleic Acids Res.*, **39**, 7750–7763.
18. Wolf,A.R. and Mootha,V.K. (2015) Functional genomic analysis of human mitochondrial RNA processing. *Cell Rep.*, **7**, 918–931.
19. Chatterjee,A., Seyfferth,J., Lucci,J., Pfanner,N., Becker,T., Akhtar,A., Panhale,A., Stehle,T., Kretz,O., Sahyoun,A.H. *et al.* (2016) Article MOF acetyl transferase regulates transcription and respiration in mitochondria article MOF acetyl transferase regulates transcription and respiration in mitochondria. *Cell*, **167**, 722–738.
20. Thul,P.J., Thul,P.J., Åkesson,L., Wiking,M., Mahdessian,D., Geladaki,A., Ait,H., Alm,T., Asplund,A., Björk,L. *et al.* (2017) A subcellular map of the human proteome. *Science*, **3321**, 1–22.
21. Luuk,H., Jønson,L., Lillev,K., Philips,M. and Vikes,J. (2009) Characterization of MYG1 gene and protein : subcellular distribution and function Biology of the Cell. *Biol. Cell*, **101**, 361–373.
22. Someya,S., Yamasoba,T., Kujoth,G.C., Pugh,T.D., Weindruch,R., Tanokura,M and Prolla,T.A. (2008) The role of mtDNA mutations in the pathogenesis of age-related hearing loss in mice carrying a mutator DNA polymerase gamma. *Neurobiol. Aging*, **29**, 1080–1092.
23. Vianna,C.R., Huntgeburth,M., Coppari,R., Choi,C.S., Lin,J., Krauss,S., Barbatelli,G., Tzameli,I., Kim,Y., Cinti,S. *et al.* (2007) Hypomorphic mutation in PGC1β causes mitochondrial dysfunction and liver insulin resistance. *Cell Metab.*, **4**, 453–464.
24. Philips,M., Abramov,U., Lilleväli,K., Luuk,H., Kurrikoff,K., Raud,S., Plaas,M., Innos,J., Puussaar,T., Kõks,S. *et al.* (2010) Myg1 -deficient mice display alterations in stress-induced responses and reduction of sex-dependent behavioural differences. *Behav. Brain Res.*, **207**, 182–195.
25. Kõks,S., Luuk,H., Nelovkov,A., Areda,T. and Vasar,E. (2004) A screen for genes induced in the amygdaloid area during cat odor exposure. *Genes Brain Behav.*, **3**, 80–89.
26. Kingo,K., Philips,M.A., Aunin,E., Luuk,H., Karelson,M., Rätsep,R., Silm,H., Vasar,E. and Kõks,S. (2006) MYG1, novel melanocyte related gene, has elevated expression in vitiligo. *J. Dermatol. Sci.*, **1**, 2–5.
27. Callebaut,I., Moshous,D., Mornon,J., Villartay,J. De and Inserm,U. (2002) Metallo- b -lactamase fold within nucleic acids processing enzymes : the b -CASP family. *Nucleic Acids Res.*, **30**, 3592–3601.
28. Arvind,L. and Koonin,E.V. (1998) A novel family of predicted phosphoesterases include Drosophila prune protein and Bacterial RecJ exonuclease. *Trends Biochem. Sci.*, **23**, 17–19.
29. Granneman,S., Kudla,G., Petfalski,E. and Tollervey,D. (2009) Identification of protein binding sites on U3 snoRNA and pre-rRNA by UV cross-linking and high-throughput analysis of cDNAs. *Proc. Natl. Acad. Sci. U.S.A.*, **106**, 9613–9618.
30. Webb,S., Hector,R.D., Kudla,G. and Granneman,S. (2014) PAR-CLIP data indicate that Nrd1-Nab3-dependent transcription termination regulates expression of hundreds of protein coding genes in yeast. *Genome Biol.*, **15**, R8.
31. Cardamone,M.D., Tanasa,B., Cederquist,C.T., Rosenfeld,M.G., Liesa,M., Cardamone,M.D., Tanasa,B., Cederquist,C.T., Huang,J., Mahdaviani,K. *et al.* (2018) Mitochondrial retrograde signaling in mammals is mediated by the transcriptional cofactor GPS2 via article mitochondrial retrograde signaling in mammals is mediated by the transcriptional cofactor GPS2 via direct mitochondria-to-nucleus translocation. *Mol. Cell*, **69**, 757–772.
32. Kuznetsova,I., Siira,S.J., Shearwood,A.J., Ermer,J.A., Filipovska,A. and Rackham,O. (2017) Simultaneous processing and degradation of mitochondrial RNAs revealed by circularized RNA sequencing. *Nucleic Acids Res.*, **45**, 5487–5500.
33. Dwivedi,M., Laddha,N.C. and Begum,R. (2013) Correlation of increased MYG 1 expression and its promoter polymorphism with disease progression and higher susceptibility in vitiligo patients. *J. Dermatol. Sci.*, **71**, 195–202.
34. Natarajan,V.T., Singh,A., Kumar,A.A., Sharma,P., Kar,H.K., Marrot,L., Meunier,J., Natarajan,K., Rani,R. and Gokhale,R.S. (2010) Transcriptional upregulation of Nrf2-dependent phase II detoxification genes in the involved epidermis of vitiligo vulgaris. *J. Invest. Dermatol.*, **130**, 2781–2789.
35. Schallreuter,K.U., Moore,J., Wood,J.M., Beazley,W.D., Gaze,D.C., Tobin,D.J., Marshall,H.S., Panske,A., Panzig,E. and Hibberts,N.A. (1999) In vivo and in vitro evidence for hydrogen peroxide (H 2 O 2) successful removal by a UVB-Activated Pseudocatalase. *J. Invest. Dermatol. Symp. Proc.*, **4**, 91–96.
36. Schallreuter,K.U., Moore,J., Wood,J.M., Beazley,W.D., Peters,E.M.J., Marles,L.K., Behrens-williams,S.C., Dummer,R., Blau,N. and Tho,B. (2001) Epidermal H2O2 accumulation alters tetrahydrobiopterin (6BH 4) recycling in vitiligo: identification of a general mechanism in regulation of all 6BH 4 -dependent processes?. *J. Invest. Dermatol.*, **116**, 167–174.
37. Singh,A., Gotherwal,V., Junni,P., Vijayan,V., Tiwari,M., Ganju,P., Kumar,A., Sharma,P., Fatima,T., Gupta,A. *et al.* (2017) Mapping architectural and transcriptional alterations in non- lesional and lesional epidermis in vitiligo. *Nat. Sci. Rep.*, **7**, 9860.
38. Calvo,S.E., Clauser,K.R. and Mootha,V.K. (2016) MitoCarta2. 0 : an updated inventory of mammalian mitochondrial proteins. *Nucleic Acid Res.*, **44**, 1251–1257.
39. Komili,S., Farny,N.G., Roth,F.P. and Silver,P.A. (2007) Functional specificity among ribosomal proteins regulates gene expression. *Cell*, **131**, 557–571.
40. Segev,N. and Gerst,J.E. (2018) Specialized ribosomes and specific ribosomal protein paralogs control translation of mitochondrial proteins. *J. Cell Biol.*, **217**, 117–126.
41. Shepard,P.J., Choi,E., Lu,J., Flanagan,L.A. and Hertel,K.J. (2011) Complex and dynamic landscape of RNA polyadenylation revealed by PAS-Seq. *RNA*, **17**, 761–772.
42. Amunts,A., Brown,A., Toots,J., Scheres,S.H.W. and Ramakrishnan,V. (2015) The structure of the human mitochondrial ribosome. *Science*, **348**, 95–98.
43. Martin,W.F., Garg,S., Zimorski,V. and Martin,W.F. (2015) Endosymbiotic theories for eukaryote origin. *Philos. Trans. R. Soc. London.*, **370**, 20140330.
44. Lucia,M., Anna,D., Urbanelli,S., Mastrofrancesco,A., Camera,E., Iacovelli,P., Leone,G., Manini,P., Ischia,M.D. and Picardo,M. (2003) Alterations of mitochondria in peripheral blood mononuclear cells of vitiligo patients. *Pigment Cell Melanoma Res.*, **16**, 553–559.
45. Lucia,M., Anna,D., Ottaviani,M., Kovacs,D., Mirabilii,S., Brown,A., Cota,C., Migliano,E., Bastonini,E., Bellei,B. *et al.* (2017) Energetic mitochondrial failing in vitiligo and possible rescue by cardiolipin. *Nat. Sci. Rep.*, **7**, 13663.
46. Prignano,F., Pescitelli,L., Becatti,M., Di,P., Lotti,T. and Fiorillo,C. (2009) Ultrastructural and functional alterations of mitochondria in perilesional vitiligo skin. *J. Dermatol. Sci.*, **54**, 157–167.
47. Pagano,G., Talamanca,A.A., Castello,G., Cordero,M.D., Ischia,M., Gadaleta,M.N., Pallardó,F.V, T,S.P., Tiano,L. and Zatterale,A. (2014) Oxidative stress and mitochondrial dysfunction across broad-ranging pathologies: toward mitochondria-targeted clinical strategies. *Oxid. Med. Cell. Longev.*, **2014**, 541230.